Technologies to Enhance Operation of the Existing Natural Gas Compression Infrastructure

Quarterly Technical Progress Report

Reporting Period Start Date: 04/01/03
Reporting Period End Date: 06/30/03

Principal Authors:

Anthony J. Smalley
Ralph E. Harris
Gary D. Bourn

July 2003

DOE Award No. DE-FC26-02NT41646
SwRI Project No. 18.06223

Submitting Organization:

Southwest Research Institute®
6220 Culebra Road
San Antonio, TX 78238-5166

DISCLAIMER

"This report was prepared as an account of work sponsored by an agency of the United States Government. Neither the United States Government nor any agency thereof, nor any of their employees, makes an warranty, express or implied, or assumes any legal liability or responsibility for the accuracy, completeness, or usefulness of any information, apparatus, product, or process disclosed, or represents that its use would not infringe privately owned rights. Reference herein to any specific commercial product, process, or service by trade name, trademark, manufacturer, or otherwise does not necessarily constitute or imply its endorsement, recommendation, or favoring by the United States Government or any agency thereof. The views and opinions of authors expressed herein do not necessarily state or reflect those of the United States Government or any agency thereof."

ABSTRACT

This report documents work performed in the third quarter of the project entitled: *Technologies to Enhance Operation of the Existing Natural Gas Compression Infrastructure*. The project objective is to develop and substantiate methods for operating integral engine/compressors in gas pipeline service, which reduce fuel consumption, increase capacity, and enhance mechanical integrity. The report describes the following work: first field test; test data analysis.

TABLE OF CONTENTS

LIST OF FIGURES

Page

1. INTRODUCTION

This report documents work performed in the third quarter (April 2003 through June 2003) of the project entitled: *Technologies to Enhance Operation of the Existing Natural Gas Compression Infrastructure*.

The project objective is to develop and substantiate methods for operating integral engine/compressors in gas pipeline service, which reduce fuel consumption, increase capacity, and enhance mechanical integrity.

The project has been structured in three phases – the first to last eighteen (18) months, with nine (9) tasks. These tasks, with their objectives, are as follows:

1. **Research Management Plan:** To define a work breakdown structure and supporting narrative that addresses the overall project objectives.

2. **Technology Status Assessment:** To describe current and competing technologies for pipeline compression, with strengths and weaknesses.

3. **Industry Advisory Committee (IAC):** To interact with industry advisors and their suppliers and, thereby, focus the work and help transfer knowledge into practice.

4. **Test Plan:** To develop a test plan which addresses project objectives, and which will serve as a basis for tests to be performed at various industry sites.

5. **Data Acquisition System (DAS):** To develop a data system which will support project objectives and acquire all needed data with appropriate format, data rates, and display.

6. **Test Program:** To perform tests on a representative series of engine/compressors; gather data to develop required relationships for efficiency, capacity, and mechanical integrity.

7. **Data Analysis:** To relate power cylinder standard deviation, balancing process, and compressor cylinder operation to fuel flow, compression efficiency, and crankshaft strain through models.

8. **Methods for Optimized Operation:** To apply the models and develop optimized methods for balancing and operating engine/compressors.

9. **Program Management:** To perform planning, administrative, and technical direction functions to achieve project objectives; to communicate with and report to the DOE and other co-funding organizations.

So far, progress has been made under Tasks 1 through 7 and Task 9, and is discussed in the subsequent sections of this quarterly report.

In the first quarter, Task 1 was completed, and progress was made on Tasks 2, 3, 4, 5, and 9.

In the second quarter, Tasks 2, 4, and 5 were completed; further progress was made on Tasks 3 and 9, and initial progress was made on Task 6 (calibration and site visit for first test site).

In the third quarter, the initial test at the first site was completed (Task 6) and data analysis was started (Task 7).

2. EXECUTIVE SUMMARY

Tasks 1, 2, 4, and 5 were completed prior to this quarter.

An Industry Advisory Committee (IAC) was formed in the first quarter. A first IAC meeting was held January 14, 2003, and provided valuable project direction. A second IAC meeting was held June 24, 2003, and provided further focus to the direction of the project. This activity falls under project Task 3.

Following an initial site visit, the first field test was held at El Paso Corporation's Station 823 in Kinder, Louisiana on a Clark HBA-6, April 15-17, 2003. This is the first major activity under Task 6.

Since the initial field test, significant analysis of data obtained during the test has been performed, as part of Task 7.

The following report discusses these items of progress in more detail.

3. EXPERIMENTAL

According to the Test Plan, the following data channels were to be acquired simultaneously and processed as part of the testing:

- *Compressor Cylinder Dynamic Pressure* - used for compressor horsepower and flow determination (Sensotec piezo-restrictive transducer).
- *Engine Dynamic Cylinder Pressure* - used for engine horsepower determination, engine balance, and engine statistics (Kistler quartz piezoelectric transducer).
- *Engine Intake and Exhaust Dynamic Pressure Measurements* - used to correlate acoustic dynamic effects to engine statistics (Kistler piezo-resistive transducer (water-cooled)).
- *Torsional Vibrations (IRV)* - used as a surrogate for mechanical integrity (BEI 512 pulse encoder).
- *Bearing Centerline Vibration Measurements* - used as a surrogate for mechanical integrity (PCB velocimeters).
- *Crankshaft Dynamic Strain* - acquired using SwRI's Strain Data Capture Module (SDCM). Used as a direct measurement of shaft loading, and used to provide link between engine statistical quantities (PFP), and crankshaft fatigue damage [Ref. 1].
- *Engine Fuel Flow* - used to document overall engine efficiency (AGA3 method using Emerson Flobas 103).
- *Suction Header and Discharge Header Pressures and Temperatures* - used for installation efficiency determination (Sensotec piezo-restrictive transducer).
- *Engine Exhaust NO_X and O_2 Levels* - used for input into an engine performance model (NGK fast-response transducer).
- *Compressor Rod Load* - used for both mechanical integrity and loading optimization (strain gage-based; bridged to cancel bending).

For the first test at TGP's Kinder, Louisiana station (April 15-17, 2003), the majority of these channels were successfully acquired as a coherent data set for every test condition. All channels were calibrated prior to the tests. In addition to the channels listed above, a

portable emissions analyzer (an ECOM A+) was used to measure concentration of NO, NO_2, NO_X, O_2, and CO in the exhaust.

A few of the channels listed above gave problems. The engine fuel flow meter was calibrated prior to the test, but it was discovered during the test that it was set for a much higher flow rate than was needed and did not give useful data. The rod load monitor RF transmitter drifted too much. This is a development device and the underlying problem has now been corrected. The power cylinder #1 pressure transducer gave suspect data, exhaust header pressure, and temperature values were also not acquired.

4. RESULTS AND DISCUSSION

INDUSTRY ADVISORY COMMITTEE (IAC) TASKS

A second meeting of the Industry Advisory Committee (IAC) was held June 24, 2003 at SwRI offices in San Antonio. All five committee members attended, as well as the three lead members of the SwRI project team. The meeting agenda was as follows:

- Project Recap
- Result from First Test
- Discussion of Test Results
- Discussion of Possible Expansion of Scope
- Selection of Second Test Site
- Next Meeting

The meeting was active, productive, and valuable. Based on the results, it was agreed that there would be value to investigating hardware solutions to an identified operating problem – namely air imbalance between power cylinders, but not at the expense of investigations planned into the existing scope. Some extension of scope will be pursued.

It was agreed that the second test site should be a GMW, with high-pressure fuel injection – at Williams Sour Lake station, with load step and load variation tests.

The return to the first site may be delayed to dovetail with plans for more extensive work to deal with air imbalance. This will be further reviewed.

TEST PROGRAM (TASK 6)

The first test at the first site (El Paso Corporation's Kinder Station 823) was completed. Data was acquired as described in the experimental section of this report. Tests were performed to investigate how compressor operation and engine balancing affect integrity and performance of the engine.

Figure 1 shows the test engine. It is a turbocharged HBA-6 with four compressor cylinders. Its rated BHP power is approximately 1680 HP (1.25 MW) and its nominal speed is 300 RPM. Close inspection of Figure 1 shows a tripod located next to the flywheel, which carries an encoder connected via a temporarily installed shaft to the flywheel. The encoder triggers analog-to-digital conversion of the pressure transducer signals at the rate of 512 samples per revolution, and also provides a pulse train from which crankshaft instantaneous rotational velocity can be determined. The air manifold pressure transducer at the flywheel end of the air manifold, just above the compressor cylinder doghouse, can also be seen in this figure.

Figure 1. Initial Site Test
(HBA-6, TGP Kinder Station)

Figure 2 shows the strain data capture module (SDCM) installed on two throws. A strain gage is glued in place close to the crank pin and oriented to measure crank web bending. The lead from the strain gage can be seen in Figure 2. The signal conditioning and data

acquisition modules can also be seen; these each contain an analog-to-digital converter, a processor, memory, and power.

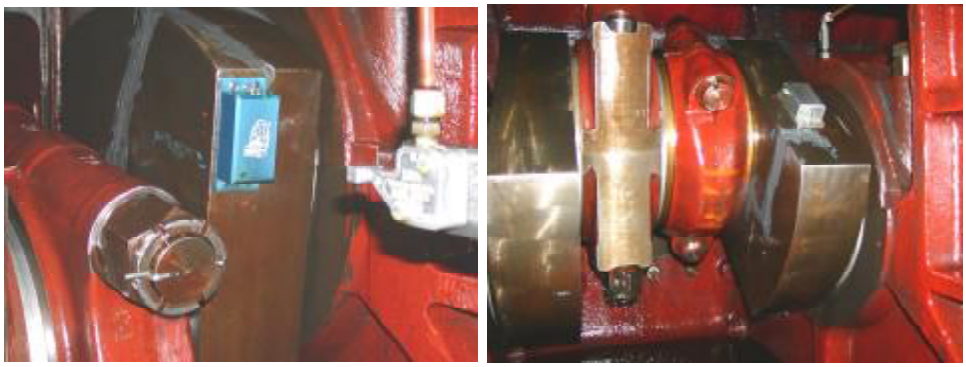

Throw 3
(Power & Compressor)

Throw 2
(Power Only)

Figure 2. SDCM Installation for Crankshaft Strain Measurements

Figure 3 shows the installation of the rod load monitor. The lead from the strain gages on the rod to the data acquisition and transmission system can be seen. As noted, this system is under development and during the test, the RF transmission system exhibited thermal drift in its transmission frequency, which made it unusable for the study. However, this problem has now been addressed and the capability should be available for subsequent tests.

Figure 3. RLM Installation

Figure 4 shows a sample of pressure data from both the power cylinders (on the left of the figure) and from the compressor cylinders (on the right). There are six traces in the power cylinder plot, but the cylinder #1 pressure transducer was suspect. These traces are averaged over 32 cycles. Even when discounting the suspect trace of cylinder #1, the spread between highest and lowest peak pressure is clear. The PFP spread in this example is 190 PSI (1.3 Mpa). This plot simply presents representative data at some stages in the test program and represents neither highest nor lowest spread. Though not shown by this figure, the cycle-to-cycle variation for any cylinder is also significant for this two-stroke engine. Because cylinder pressure varies with time and across cylinders, it is important to distinguish how spread is expressed. The *Data Analysis* section will refer to the "average instantaneous spread," which is the difference between the maximum and minimum peak-firing pressure across the cylinders in one engine revolution averaged over many cycles. The *Data Analysis* section will also refer to the average peak-firing pressure spread, which is the difference between maximum and minimum pressure as shown by the time averaged pressure in each cylinder.

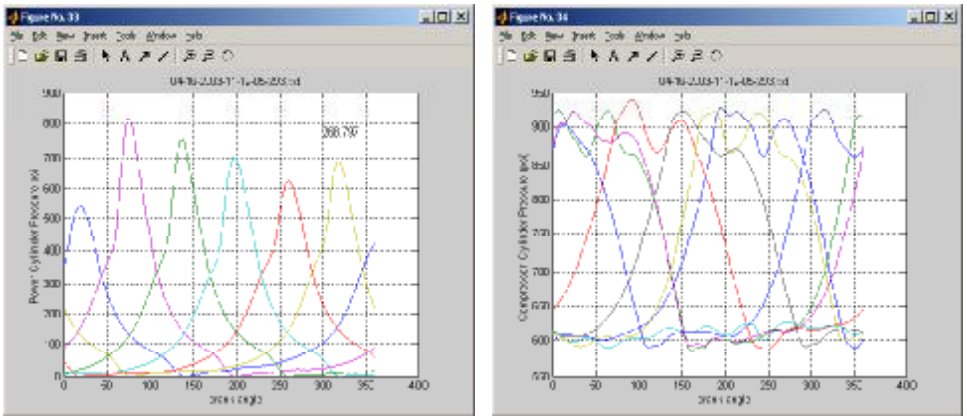

Power Cylinder Pressures Compressor Cylinder Pressures

Figure 4. Typical Data Sets

The compressor cylinders exhibit less spread between highest and lowest peak pressure. This is, in part, because discharge pressure pegs the highest cylinder pressure quite closely, and possibly because closer attention is paid to control of compressed gas acoustic pulsations outside the compressor cylinders than to air pulsations outside the

power cylinders. Close examination shows five compressor traces – this represents head and crank end from two cylinders and head end only for one cylinder. The crank end of one cylinder was deactivated, which is one convenient means of capacity control, but may not be the most efficient. This question of efficient capacity control will be considered in subsequent data analysis, which has not been completed yet.

Further typical data is shown in Figure 5. Here, we see the inlet air manifold pressure (on the left) and the crankshaft rotational velocity (on the right). Both these quantities are presented in the upper frames as the variation with crank angle from zero to 360 degrees, and in the lower frame as a spectrum showing variation with engine order from one to one hundred. The inlet air manifold pressure clearly varies quite widely over one revolution (1.8 PSI or 12.4 Kpa peak-to-peak variation out of about 7.8 PSI or 53.8 Kpa). The spectrum shows significant content out to at least the 13th order. This specific measurement was taken at the flywheel end of the air manifold (see Figure 1).

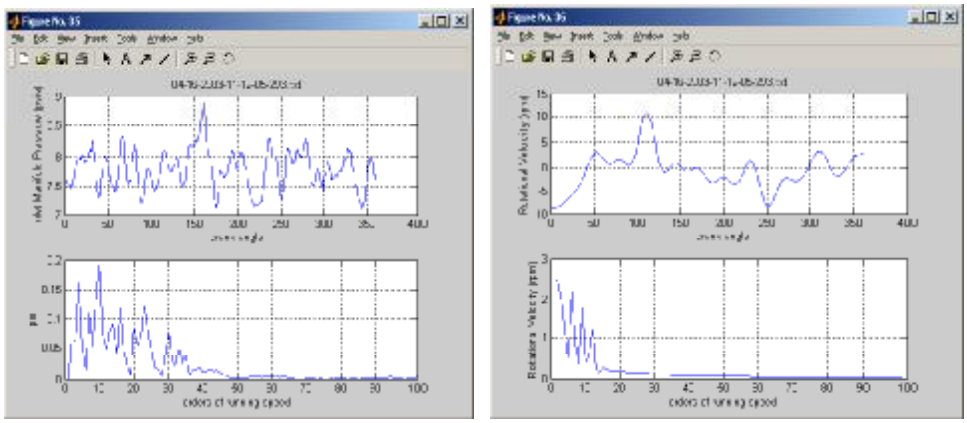

Inlet Air Manifold Pressure Rotational Velocity

Figure 5. Typical AMP and IRV Data Sets

The crankshaft velocity varies in one revolution by over 18 RPM peak-to-peak out of an average of about 300 RPM (6% variation). The spectral content of this variation is mainly concentrated in the first 12 orders.

Figure 6 presents further quantification of air manifold pressure (AMP or MAP) variation over 36 successive data sets acquired with different engine balance conditions. The average peak-to-peak variation is about 25% of the average, and it ranges from 22.6% to 26.9%. This AMP variation could be a significant contributor to imbalance or spread between cylinders, as will be subsequently discussed.

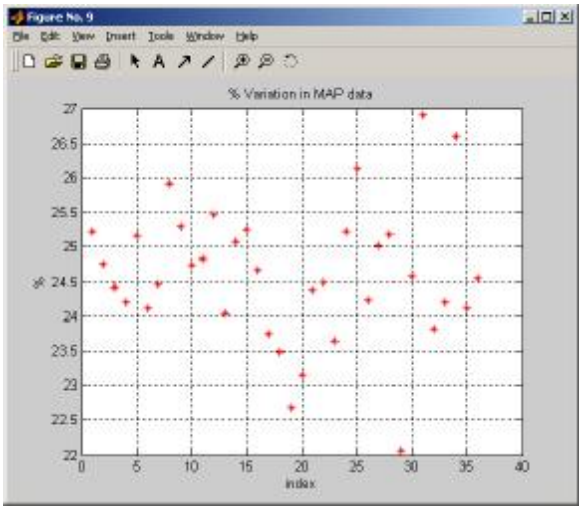

Figure 6. AMP Variation Summary

Figure 7 shows compressor differential indicated power (DIP) for head and crank ends of the compressor in percent of indicated power. DIP is a measure of the cylinder power lost to flow resistance; thus, low DIP leads to high thermal efficiency, and based on these DIP values between 3.5 and 5.5%, the efficiency would be expected to be high.

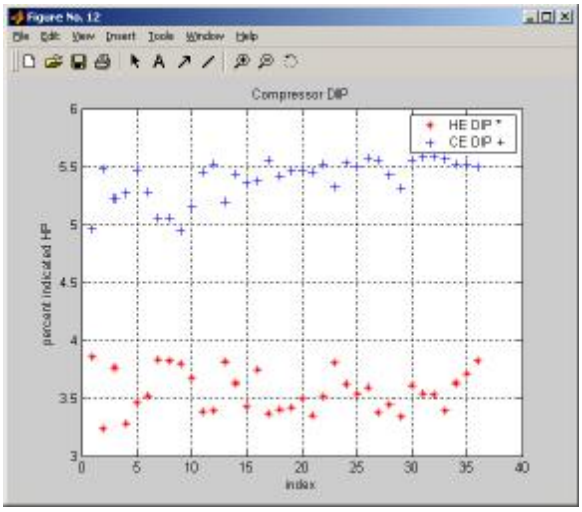

Figure 7. Compressor Performance Data
(Head and Crank End DIP)

Figure 8 confirms this – efficiencies across 36 data sets range from a low of 90.7% to a high of 91.5%. A compressor thermal efficiency survey conducted by SwRI for GMRC a few years ago, based on measured enthalpy rise, showed that 91 or 92% was about the best achieved on any pipeline industry compressor. The median thermal efficiency for the pipeline industry, based on this survey, was about 80%.

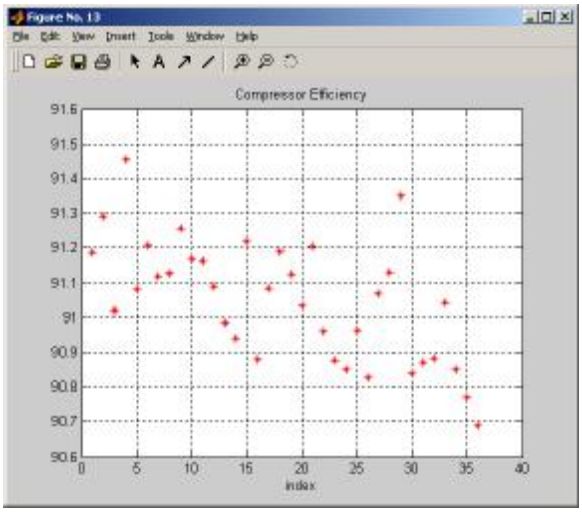

Figure 8. Compressor Efficiency Data

Thus, based on the cylinder pressure data and differential power, the compressor tested is operating at a high percentile efficiency for the industry. This is a significant positive result for three reasons: 1) it represents efficient use of fuel gas; 2) it helps lower the ratio of emissions to useful compression power; and 3) it leads to high available capacity; if at any time a compressor's capacity is limited because the load on the engine is at the safe limit for that engine, then any losses in the compressor represent engine capacity, which is unavailable as useful energy to be imparted to the transported gas. This compressor has maximized the engine capacity available for gas energy.

Figure 9 shows typical waveforms of crankshaft dynamic strain from the strain data capture module – one from a crank throw with both power and compressor cylinders acting on its crank pin, and one from a crank throw with only a power cylinder acting on its crank pin. The two second snapshots in this figure cover about 10 revolutions and show significant differences, by almost a factor of two in the magnitude of the peak-to-peak variation in strain experienced by the two crank throws. This represents significant non-uniformity along the crankshaft in the potential for fatigue damage as the crankshaft transmits power to the compressor cylinders.

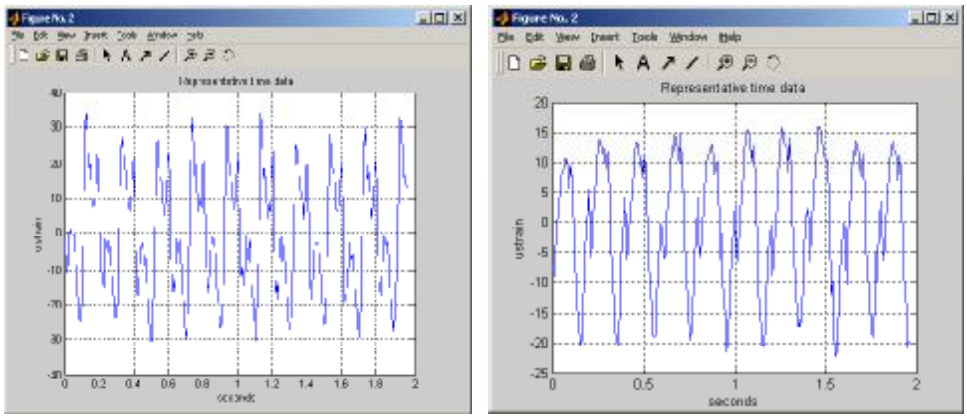

Throw 3 (Power & Compressor)

Throw 2 (Power Only)

Figure 9. Typical SDCM Waveform

Figure 10 shows the variation in peak-to-peak microstrain from the SDCMs on the same two throws over a 10-hour test period. Here, a further difference between the power and compressor throw and the power only throw becomes apparent – the throw which drives a compressor throw directly, experiences pronounced spikes in the strain, which differ in magnitude from the normal variation. The throw, which carries a power cylinder connecting rod, does not exhibit such distinct "spikiness".

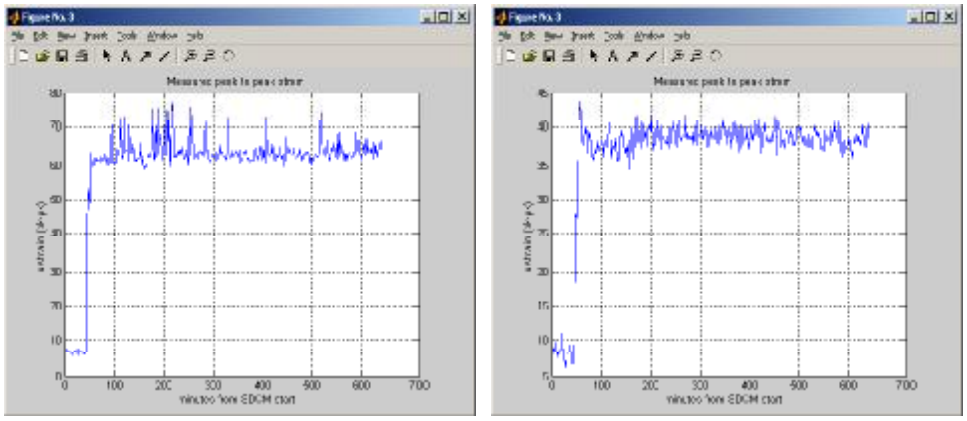

Throw 3
(Power & Compressor)

Throw 2
(Power Only)

Figure 10. Overall Peak-to-Peak Strain Summary

Figure 11 shows the variation in the strain spectra from these two throws over the period of the test. Of primary interest, here is the higher relative magnitude of second and third orders in the strain from the combination throw as opposed to the power only throw.

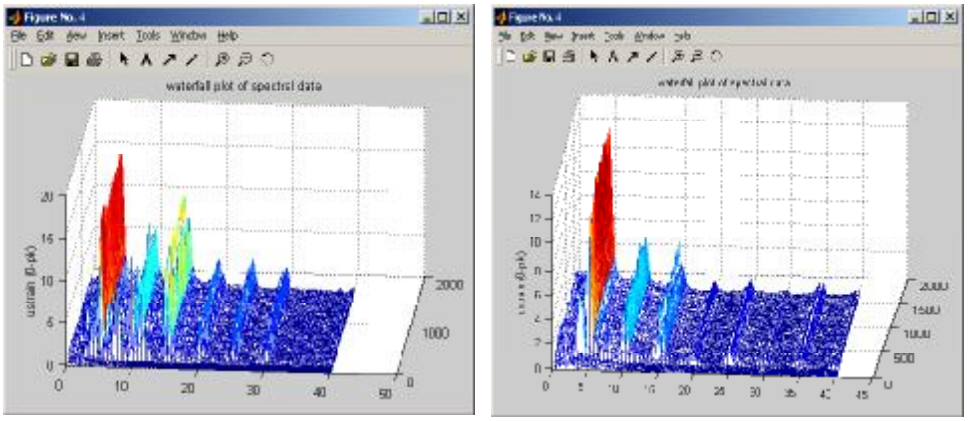

Throw 3
(Power & Compressor)

Throw 2
(Power Only)

Figure 11. Raster Plots of SDCM Data

Figure 12 compares these orders again over the 10+ hours of testing; similar observations may be made from Figure 12, as for Figure 11.

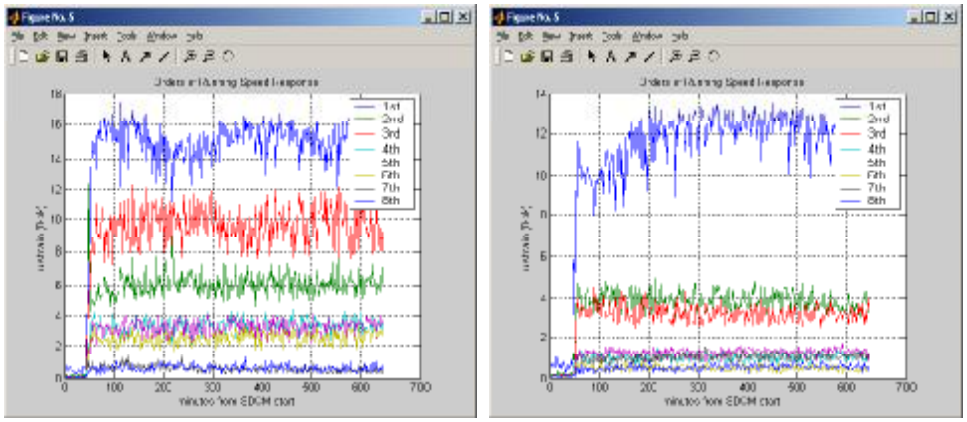

Throw 3
(Power & Compressor)

Throw 2
(Power Only)

Figure 12. Order Summary of SDCM Data

The above data are representative of what was observed during the tests. A data report CD, with power cylinder pressures, compressor cylinder pressures, AMP and IRV variation has been prepared as a deliverable, and will be transmitted to DOE pending IAC

approval. These typical data and the analyses discussed in the next report section were presented to a meeting of the IAC on June 24, 2003.

DATA ANALYSIS (TASK 7)

The significance of crankshaft strain variation is difficult to define on an absolute basis, because laboratory fatigue data does not exist for the materials out anywhere close to the number of cycles to which a crankshaft is exposed over its lifetime (over 4.5×10^9 revolutions for a 250,000-hour crankshaft). In essence, the long life crankshafts are the fatigue testers! The simple assumption in classical fatigue analysis is that an endurance limit exists – according to this assumption, if dynamic strains are below the endurance limit, then the component in question will last forever. Data makes it clear for most materials that the variation of cyclic stress amplitude with cycles to failure at that amplitude (the SN diagram) becomes flatter when the number of cycles exceeds about 10^7, but whether it is truly flat or just has a gentle slope is not clear. One explanation for the observed fact that some high hour crankshafts eventually fail is the existence of a gradual slope in the SN diagram.

To calculate possible life implications of the measured strain data, Figure 13 shows histograms of stress level for the two measured throws. These histograms give the frequency of occurrence, using a method called "rainflow counting" of different strain ranges in a two-second sample. The power/compressor combination throw clearly produces several stress cycles at nearly twice the highest stress level compared to the power only throw.

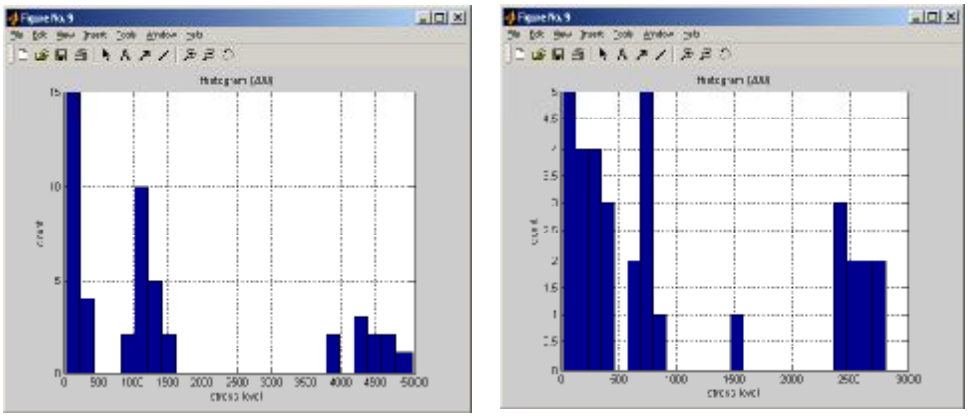

Throw 3
(Power & Compressor)

Throw 2
(Power Only)

Figure 13. Sample Histogram of Stress Reversals
(2-Second Interval)

Figure 14 seeks to show the potential implication in life of the stress level and occasional spikes from the combination throw compared to the "power only" throw. It assumes a gradual slope to the long life portion of the SN diagram with slope guided by experience on a few long life shafts. It is emphasized that this figure does not provide absolute information, just comparison. The hours to failure for the power-only throw are projected at least one thousand times the hours to failure for the power/compression combination. The spikes produce momentary damage accumulation, such that if the engine were always to run under this momentary condition, life would be reduced by a factor of more than 10. Thus, the potential life implications of the observed stress levels could be significant, but are not in themselves conclusive.

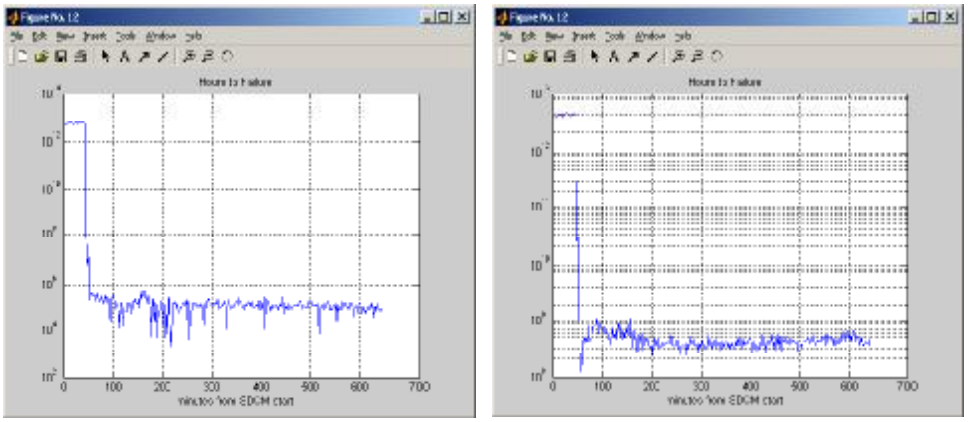

Throw 3
(Power & Compressor)

Throw 2
(Power Only)

Figure 14. Comparative Life Estimate

Figure 15 shows a typical record with strain higher than 70 microstrains.

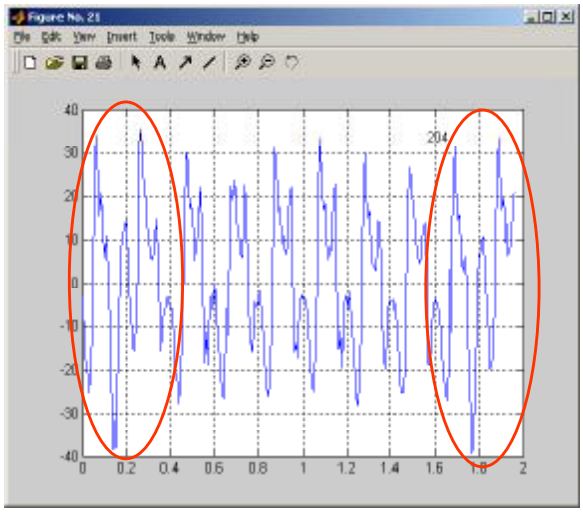

Throw 3
(Power & Compressor)

Figure 15. Sample Record with Peak-to-Peak Strain > 70

The relationship of possible cyclic strain damage to the state of engine balance was explored during the tests. Figure 16 shows the changes in average peak-firing pressure spread and the variation in average instantaneous spread during a six-hour test period in which various balancing strategies were investigated. The various timing and balancing

approaches (peak-firing pressure (PFP) balancing and coefficient of variance (COV) balancing) are noted. PFP balancing, starting just after 10:09 AM, reduces the average PFP spread almost by a factor of two, but only has a small (20%) relative influence on reducing the average instantaneous spread. Increasing the timing to 13 degrees BTDC enabled further reduction in average PFP spread to about 80 PSI. Turning all fuel valves open 100% increased both measures of spread to 250 and 300 PSI, respectively. Again, PFP balancing from this condition, now with timing at 14 degrees BTDC, reduced average PFP spread to about 75 PSI. At 1:14 PM, COV balancing (increasing fuel flow to the cylinders with highest COV for cycle-to-cycle variation) increased both measures of spread, but reduced the difference between them.

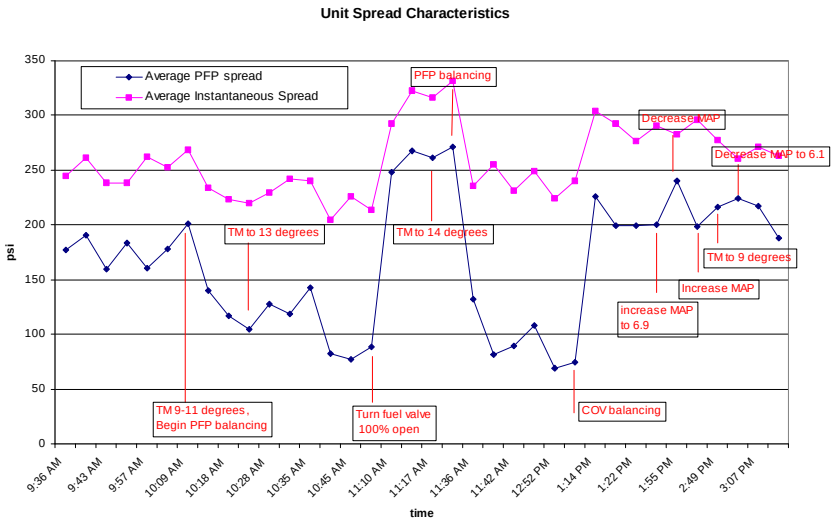

Figure 16. Unit Peak-Firing Spread Test Characteristics

In Figure 17, a measure of the "smoothness" of the crankshaft dynamic stress variation is plotted against time. This measure is referred to as T70 and equals the time in minutes since the previous crankshaft dynamic stress above 70 microstrains is observed. Also in Figure 17 is the difference between instantaneous and average PFP spread values, which provides an intuitive measure of the smoothness of operation. Both PFP and COV balancing lead to evidence of increased time between high strain events.

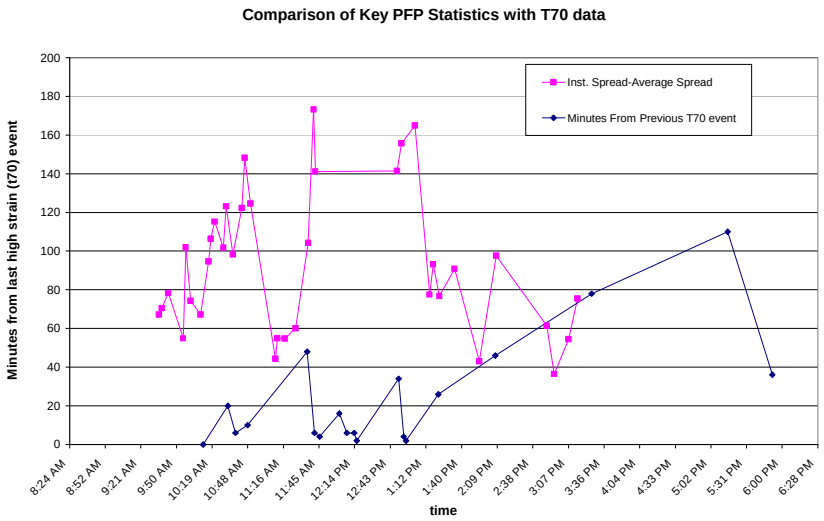

Figure 17. Comparison of Key PFP Statistics

COV balancing provides clear evidence of an improvement in engine smoothness. Unfortunately, the ability to pursue COV balancing was limited by the available range in fuel valve adjustments coupled with air imbalance, which will be discussed further below after vibration is discussed.

Figures 18 and 19 present bearing centerline vibration on the flywheel and oil pump ends of the unit as raster plots. These signals stay remarkably constant during the changes in balance approach and spread discussed previously, and therefore do not appear promising as measures of severity of conditions.

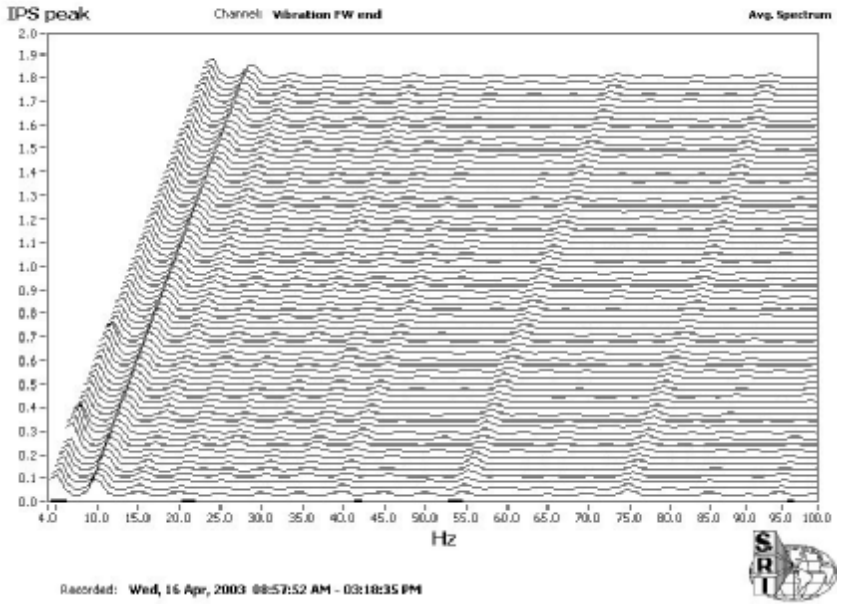

Figure 18. Vibration Bearing Centerline (Throw 1)

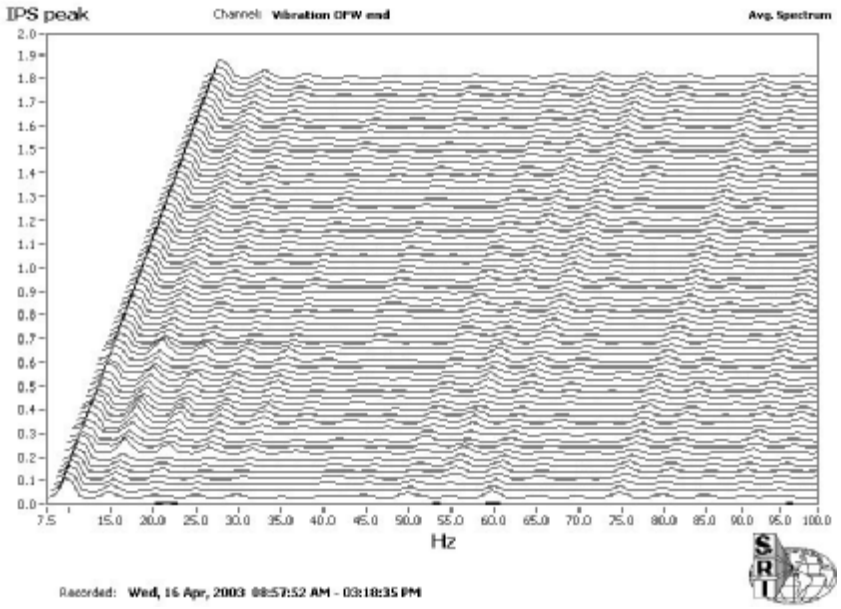

Figure 19. Vibration Bearing Centerline (Throw 6)

Figure 20 presents crankshaft instantaneous rotational velocity (IRV) as a raster plot. There appears to be slightly more variation during the changes in balance condition, but

finding a distinguishing feature, which could provide an assessment of severity of condition from the IRV, is not obvious. Figure 21 presents the peak-to-peak IRV variation in RPM during the changes in balance condition. Again, it will be difficult to extract a distinguishing measure of severity from the peak-to-peak IRV variation.

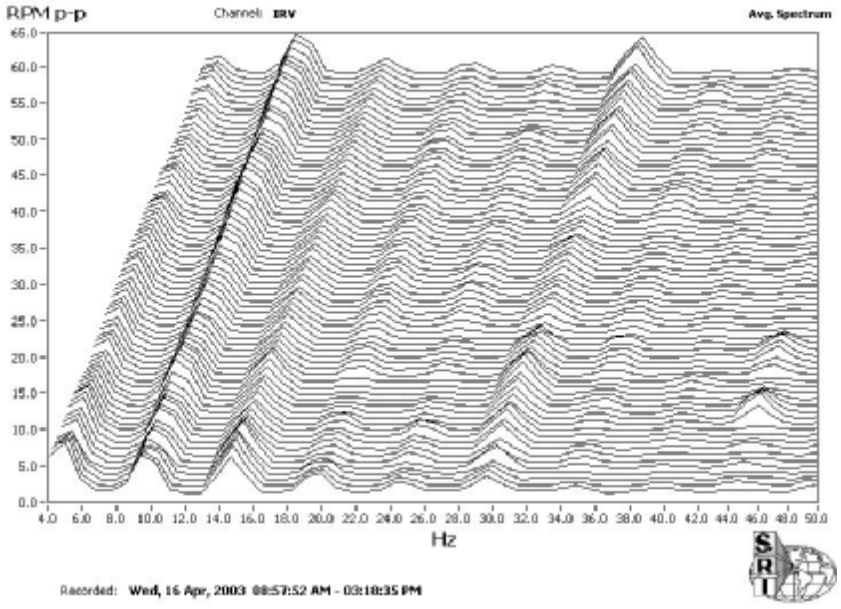

Figure 20. Crankshaft Rotational Velocity

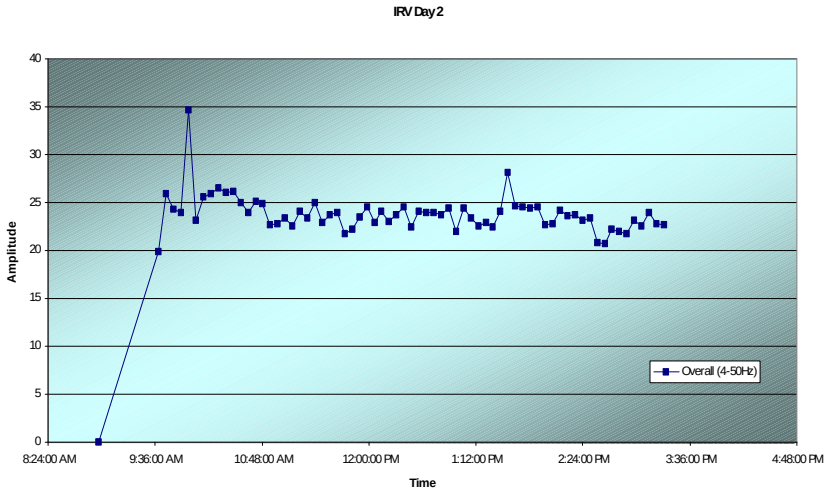

Figure 21. Summary Crankshaft Rotational Velocity

By comparison to the vibration and IRV data, the strain data capture module results clearly provide a more sensitive measure of severity of dynamic loading and potential damage.

Close review of the power cylinder pressure plots during balancing revealed a spread between the "compression pressure" values. This is the pressure developed prior to ignition as a result of compression of trapped air and fuel by piston motion following port closure. A spread in this pressure implies a different mass of trapped air (air imbalance) in the power cylinder, and also represents a different point from which pressure builds as result of heat release after ignition. Figure 22 shows traces from power cylinders 2 through 5 and makes clear the spread of 10% or more in compression pressure. Figure 22 also shows how the PFP spread is greater than the compression pressure spread, and how the PFP does not necessarily correlate with compression pressure.

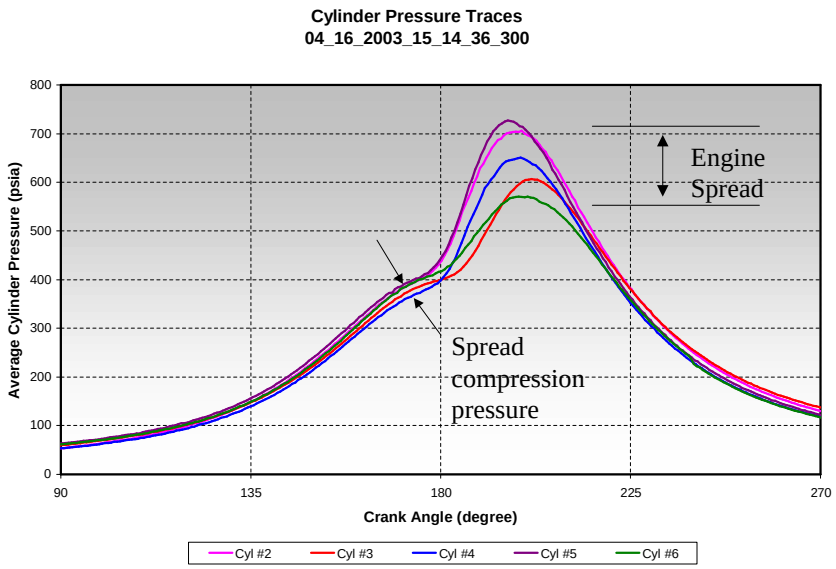

Figure 22. Sample HBA-6T Cylinder Test Data

Figure 23 shows the compression pressure for five power cylinders and its variation through 36 samples covering more than six hours of testing with different balance conditions. The cylinders clearly track each other closely in compression pressure.

Although not explicitly shown in Figure 23, the data shows that compression pressure does not exhibit the cycle-to-cycle variation that the PFP shows. The compression cylinder spread is a repeatable characteristic of the engine. Balancing to achieve equal PFP has to compensate in fuel flow for these inherent differences between cylinders.

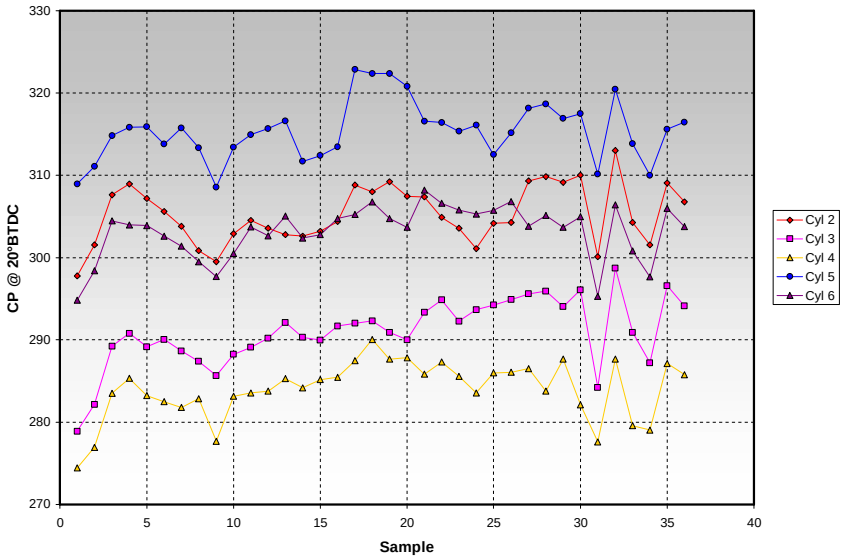

Figure 23. HBA-6T Test Data, Cylinder Pressure 20 Degrees Before TDC (Compression Pressure)

The potential reasons for the cylinder-to-cylinder variation include:

- Manifold Dynamics
- Differences in Liner Port Flow Area or Coefficient
- Compression Ratio Variation Due to Dimensional Differences in Pistons, Heads, and Liners
- Excessive Blow-By
- Variations in Crankshaft Rotational Velocity Over the Cycle

These all need to be assessed. However, it will be recalled that air manifold pressure at the measurement location exhibited a 25% variation over each revolution, as shown in Figure 5. This implies a similar spatial variation in air manifold pressure. The local air

manifold pressure drives air flow through the ports into the cylinder. Inevitably, air flow is a significant contributor to the cylinder-to-cylinder variability in trapped air mass, and therefore in compression pressure, so air manifold dynamics are a likely candidate for the primary cause of compression pressure difference.

To assist understanding of engine characteristics observed during the tests, a single cylinder combustion model was applied to this and adjusted to fit observed burn rate characteristics of the average cylinder. The cycle simulation model utilized is based on prior models developed specifically for two-stroke spark-ignited integral engines [2].

This model was then applied to assess the sensitivity of fuel consumption and emissions to changes in trapped air in the cylinder. These changes in trapped air were achieved by changing air manifold pressure. A constant pressure ratio (intake/exhaust) was assumed. While no exhaust pressure measurements were taken, previous data on another straight six indicated a closely constant pressure ratio at a constant engine speed. Empirical relationships for burn rate and combustion efficiency were based on the HBA-6 data.

The NO_X model is based on a rate formation model and tuned to the HBA data. The heat transfer model is based on the correlation by Woschni, and also tuned to the HBA data. With these tuned models, the first law of thermodynamics is used to determine cylinder temperature, then pressure. Figure 24 compares model predictions with time-averaged measured pressure averaged across the cylinders. This closely agreeing model is used in the following figures to explore the sensitivities discussed above.

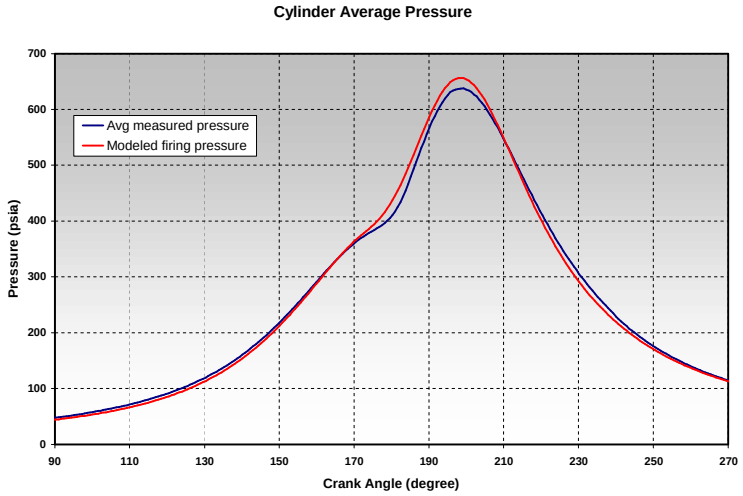

Figure 24. Comparison of Measured and Predicted Cylinder Pressure

Figure 25 shows variation of brake thermal efficiency with compression pressure if air fuel ratio is adjusted to keep peak-firing pressure constant. Figure 26 shows the required air fuel ratio adjustment to accomplish this for the same range of compression pressure and the corresponding predicted variation in NO_X. The linearity of efficiency variation and the nonlinearity of the predicted NO_X are apparent.

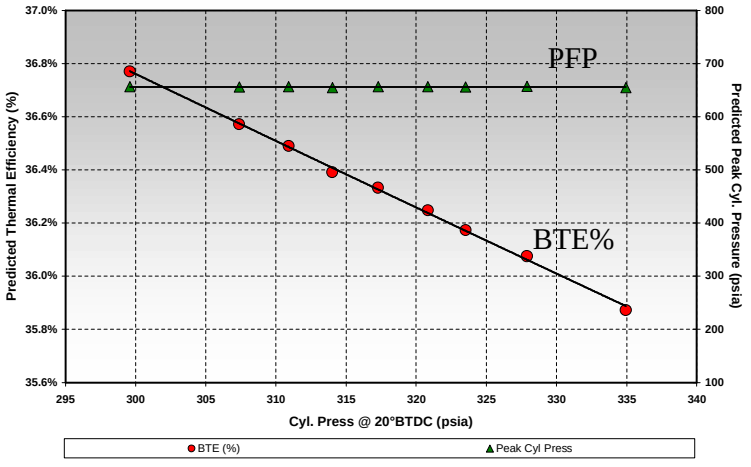

Figure 25. Effect of AMP Variation with Constant Peak Pressure – Single Cylinder Results

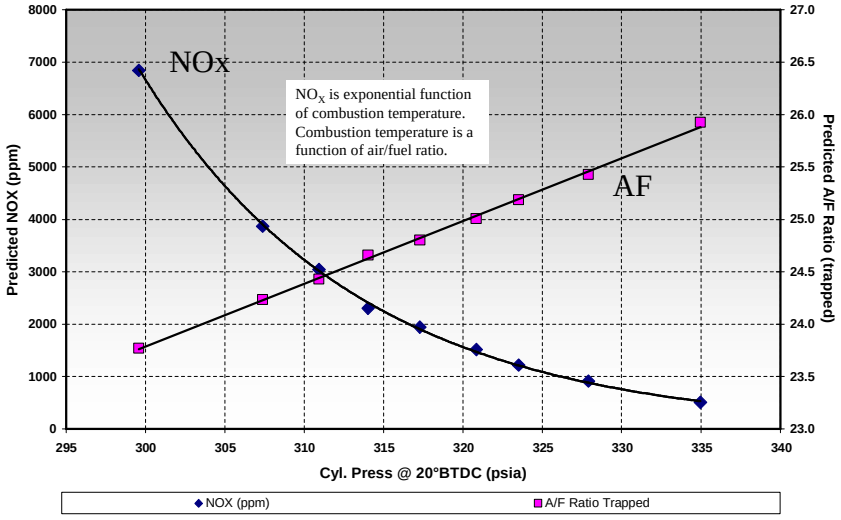

Figure 26. Effect of AMP Variation with Constant Peak Pressure – Single Cylinder Results

Figures 27 and 28 show how peak-firing pressure, brake thermal efficiency, and NO_X vary with compression pressure when air fuel ratio (also shown in Figure 28) is maintained constant.

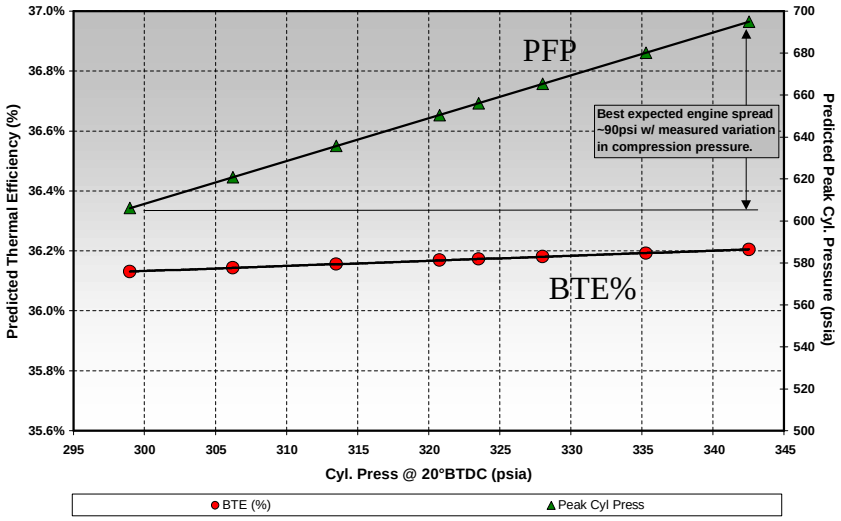

Figure 27. Effect of AMP Variation with Constant A/F Ratio – Single Cylinder

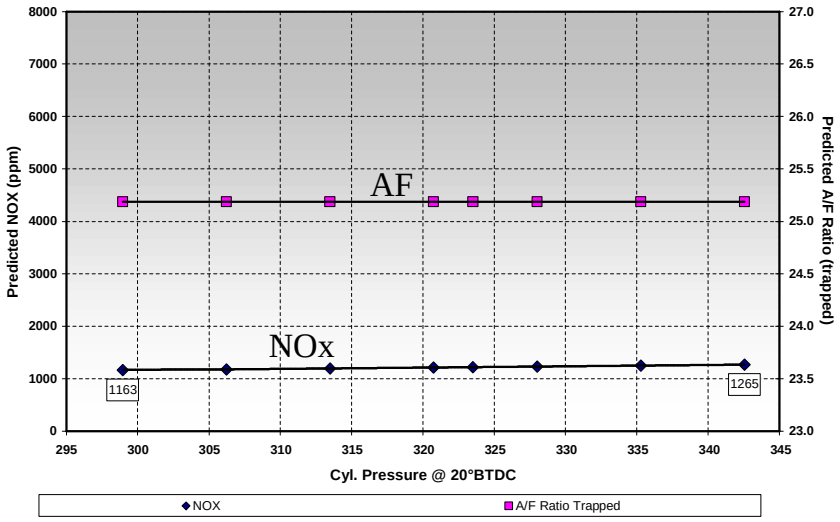

Figure 28. Effect of AMP Variation with Constant A/F Ratio – Single Cylinder Results

The single cylinder data of the preceding figures was used to predict performance of a six-cylinder engine in which the air manifold pressure driving air into the cylinders was assumed to have an evenly distributed range from high to low across the six cylinders. The fuel flow (or air fuel ratio) was adjusted to achieve constant peak-firing pressure in this engine. The performance with this engine condition is compared to the engine condition in which the air manifold pressure is constant across all cylinders, the air fuel ratio is also constant, and as result of this desirable condition peak-firing pressure is constant across the cylinders. Figure 29 shows the predicted cylinder pressure variation for the engine with evenly distributed air manifold pressure; the compression pressure has a 35 PSI spread as a result, but the peak-firing pressure is kept constant by the differences in air fuel ratio across the cylinders.

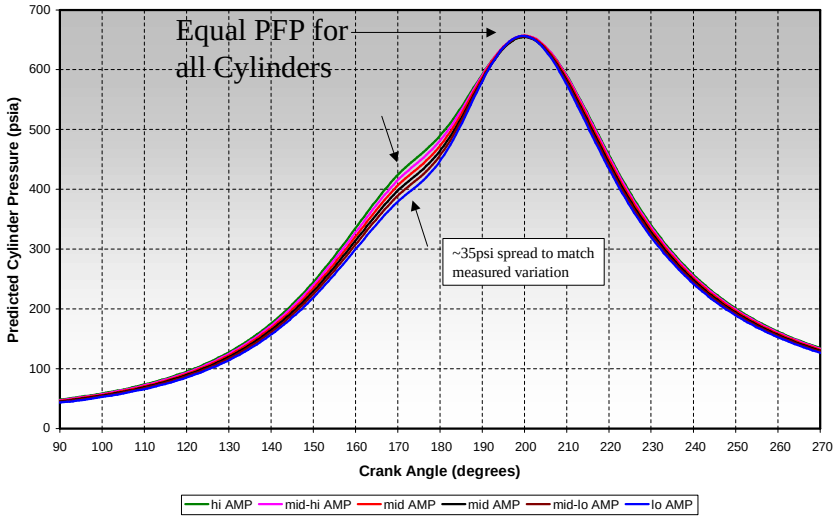

Figure 29. Predicted Cylinder Pressures – for Evenly Distributed Air Manifold Pressure - Simulation

Figure 30 shows the distributed air fuel ratios and the constant air fuel ratio values for the two "balanced" engine conditions being compared. Figure 31 compares predicted NO_X and BSFC (BTU/HP-hour) for these two engine conditions. Maintaining constant air fuel ratio is predicted to reduce NO_X by about 30% compared to the process of adjusting air fuel ratio to compensate for the variation in compression pressure, and so to achieve the same PFP. The predicted BSFC is also reduced, but by a smaller amount.

This simulation has thus far not considered the efficiency and emissions of an "un-balanced" engine where the PFP spread is very large. The reduction in NO_X emissions and fuel consumption by reducing the PFP spread, even with a spread in compression pressure, will be significant. Therefore, traditional balancing of PFP is necessary to maintain emissions compliance, and this simulation shows that further gains are possible by equalizing the cylinder-to-cylinder air flow or trapped mass. The contributions of improved mixing and other in-cylinder technology enhancements are also critical factors in reducing emissions and fuel consumption. Their benefit will, however, be maximized for cylinders with optimized air balance.

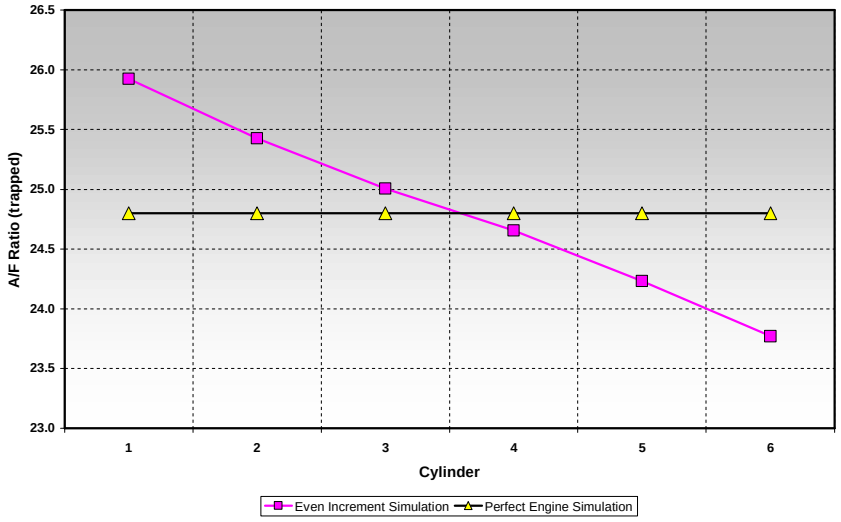

Figure 30. A/F Ratio Required for Constant Peak-Firing Pressures

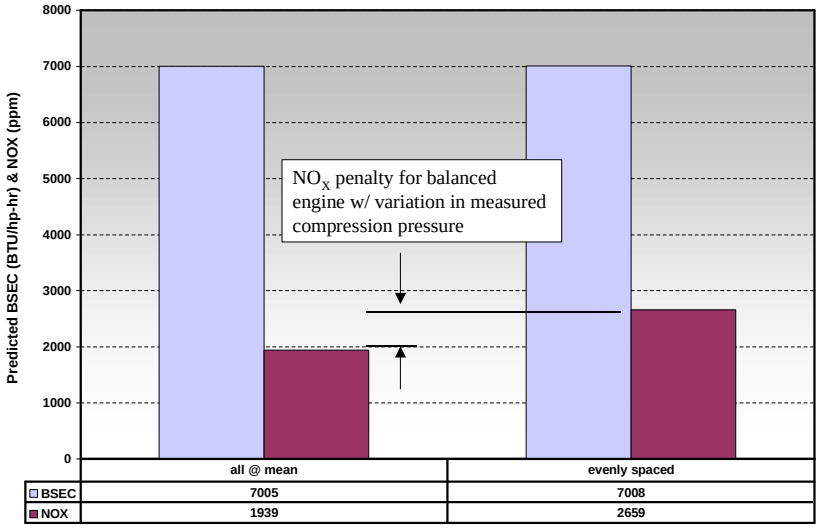

Figure 31. Balanced Engine Simulation Comparison

Thus, as a minimum, this analysis shows potential to increase NO_X compliance margin while not hurting fuel efficiency in engines with cylinder-to-cylinder variation in compression pressure. In fact, the benefit of the constant air fuel ratio condition to BSFC in this analysis may be understated, because the analysis considers no effects of cycle-to-cycle variation. Maintaining the same ideal air fuel ratio across cylinders is also expected

to minimize extremes of misfires and detonations, as part of the cycle-to-cycle variation, and thereby in practice should achieve lower BSFC.

Constant air fuel ratio in all cylinders is a more difficult balancing target to define in practice than balancing on peak-firing pressure. The COV balancing target explored during the test program is a possible surrogate. A cylinder with higher COV than others is likely too lean, and increasing fuel on high COV cylinders to bring all COVs closer together is arguably an approximate surrogate for seeking equal air fuel ratio in each cylinder.

A potential alternative surrogate for air fuel ratio balancing would be to balance on the basis of pressure rise from compression pressure to peak-firing pressure – accounting for the natural relationship of PFP to compressor pressure with constraint A/F ratio. This will be analyzed further.

The above presents the essence of the analysis performed to date on the data acquired during the first test at the first site. Further data analysis is planned to address compressor and system efficiency and system capacity, and to add further to the engine performance data.

An alternative to balancing on air fuel ratio to account for spread in compression pressure is to reduce this spread. This will require control of air manifold flow and dynamics. Plans for a supplementary effort to accomplish this through physical modifications to the air manifold are in preparation.

5. CONCLUSIONS

Data so far leads to some observations of potential significance if they can be exploited by beneficial changes in practice:

- Minimizing the averaged peak-firing pressure spread provides an easily defined target for engine balancing, but with variations in compression pressure, it needs some supplementing to further optimize engine performance.

- Making changes to the air system, which eliminate the cylinder-to-cylinder variation in compression pressure, has the potential to improve engine operation, make peak-firing pressure balancing more effective, improve integrity, and reduce emissions without a corresponding increase in fuel consumption. The contributing role of dimensional differences in power assembly components and speed variations need to be determined in the process.

- A balancing method, which achieves constant air fuel ratio, is a desirable target for engines with spread in compressor pressure, and should be explored further.

- The compressor tested has a high thermal efficiency (around 91%). The benefit of achieving such efficiency compared to 80% (the industry median from a GMRC study) is over 13% increase in the engine power available for useful compression, and therefore a 13% increase in capacity on days of high demand.

6. REFERENCES

[1] Harris, R.E., Edlund, C.E., Smalley, A.J., and Weilbacher, G., "Dynamic Crank Web Strain Measurements for Reciprocating Compressors," presented at the GMRC Gas Machinery Conference (GMC), October 2-4, 2000, Colorado Springs, Colorado.

[2] Wood, C.D. and Kubesh, J.K., "Evaluation of Emissions Control Technology for Reciprocating Integral Engine-Compressor Units," SwRI Report for Tenneco Gas Environmental and Technology Department, May 1995.

7. LIST OF ACRONYMS AND ABBREVIATIONS

A/F	Air/Fuel Ratio
AGA	American Gas Association
AMP	Air Manifold Pressure
BEI	Manufacturer's Trade Name
BSFC	Brake Specific Fuel Consumption
CO	Carbon Monoxide
COV	Coefficient of Variance
DAS	Data Acquisition System
DIP	Differential Indicated Power
DOE	U.S. Department of Energy
ECOM A+	An Emissions Analyzer Model
GMC	Gas Machinery Conference
GMRC	Gas Machinery Research Council
GMW	Pipeline Engine Model
HBA-6	Clark Engine Model
HP	Horsepower
IAC	Industry Advisory Committee
IRV	Instantaneous Rotational Velocity
Kpa	Kilo Pascals
MAP	Manifold Air Pressure (=AMP)
Mpa	Mega Pascals
MW	Megawatts
NGK	Manufacturer's Trade Name
NO	Nitric Oxide
NO_2	Nitrous Oxide
NO_X	Oxides of Nitrogen
O_2	Oxygen Molecule
PCB	Manufacturer's Trade Name
PFP	Peak-Firing Pressure
PSI	Pounds Per Square Inch
RF	Radio Frequency
RLM	Rod Load Monitor
RPM	Revolutions Per Minute
SDCM	Strain Data Capture Module
SN	Stress *vs.* Number of Cycles to Failure
SwRI®	Southwest Research Institute®
TGP	Tennessee Gas Pipeline